



**HAL**  
open science

## Protein-Silica Hybrid Submicron Particles: Preparation and Characterization

Jaime Vega-Chacón, Mohamad Tarhini, Nouredine Lebaz, Miguel Jafelicci, Nadia Zine, Abdelhamid Errachid, Abdelhamid Elaissari

► **To cite this version:**

Jaime Vega-Chacón, Mohamad Tarhini, Nouredine Lebaz, Miguel Jafelicci, Nadia Zine, et al.. Protein-Silica Hybrid Submicron Particles: Preparation and Characterization. *Chemistry Africa*, 2020, 3, pp.793-801. 10.1007/s42250-020-00138-3 . hal-02554148

**HAL Id: hal-02554148**

**<https://hal.science/hal-02554148>**

Submitted on 13 Nov 2023

**HAL** is a multi-disciplinary open access archive for the deposit and dissemination of scientific research documents, whether they are published or not. The documents may come from teaching and research institutions in France or abroad, or from public or private research centers.

L'archive ouverte pluridisciplinaire **HAL**, est destinée au dépôt et à la diffusion de documents scientifiques de niveau recherche, publiés ou non, émanant des établissements d'enseignement et de recherche français ou étrangers, des laboratoires publics ou privés.

# Protein-Silica Hybrid Submicron Particles: Preparation and Characterization

Jaime Vega-Chacón<sup>1,2</sup> · Mohamad Tarhini<sup>1</sup> · Nouredine Lebaz<sup>1</sup> · Miguel Jafelicci Jr<sup>2</sup> · Nadia Zine<sup>1</sup> · Abdelhamid Errachid<sup>3</sup> · Abdelhamid Elaissari<sup>1</sup>

## Abstract

**Purpose** Hybrid nanoparticles are an interesting type of particles currently employed in nanomedicine. They can combine the therapeutic and diagnostic functions of their components into one single nanosystem and therefore, can be tweaked according to their applications and desired results. The purpose of this work is to develop an easily tuned nano-system of bovine serum albumin-silica hybrid nanoparticles.

**Methods** BSA nanoparticles were prepared by nanoprecipitation process using water as the solvent phase and ethanol as the non-solvent. Silica was produced through a sol-gel process and deposited inside the BSA nanoparticles via template deposition. The effect of initial concentrations of raw materials on the structure and colloidal properties of the system was evaluated using FTIR, TGA, TEM, and zeta potential measurements.

**Results** A hybrid structure of BSA-silica was obtained. The results suggest that the particles size, isoelectric point and silica content of the hybrid nanoparticles can be easily tuned by controlling adequately the concentration of TEOS and ammonia.

**Conclusion** Our method can be considered as a novel approach for hybrid nanoparticle synthesis. To our knowledge, we report for the first time the synthesis of silica-BSA hybrid particles with a non-core-shell structure. In addition, we proved that the particles size, isoelectric point and silica content of the hybrid nanoparticles can be easily tuned by controlling adequately the concentration of TEOS and ammonia.

**Keywords** BSA · Silica · Hybrid nanoparticles · Characterization

## 1 Introduction

The preparation of nanoparticles is a research field which had a high technological development and commercial interest during the last decades due to the production of materials with unique properties that have been widely employed. Particularly, in the biomedical and pharmaceutical domains, the preparation of nanoparticles has received considerable attention owing to their capacity of interacting intimately

with biological structures [1]. Thereby, nanoparticles have been used as delivery systems (drugs, genes, proteins) [2–4], therapeutic agents (photothermal therapy, magnetic hyperthermia therapy, photodynamic therapy) [5–7] and imaging agents (magnetic resonance imaging, fluorescent imaging) [8, 9], exhibiting good results under biological conditions. Nanoparticles can be synthesized from different materials such as polymers, metals, oxides, chalcogenides. In other cases, hybrid nanoparticles can be made with more than one base material [10–13]. Some hybrid nanoparticles combine synergistically the therapeutic and diagnostic functions of their components into a single nanosystem, improving the efficiency of diseases treatment. In addition, the presence of different materials in a single system allows the interaction between them and may lead to changes in properties such as colloidal stability, chemical stability, biodegradability, carrying capacity, toxicity. Hybrid nanoparticles represent a promising strategy for the detection and treatment of cancer and other diseases [14–17].

---

✉ Mohamad Tarhini  
mohamad.tarhini@univ-lyon1.fr

1 University Lyon, University Claude Bernard Lyon-1, CNRS, LAGEPP-UMR 5007, 43 Boulevard du 11 Novembre 1918, 69100 Villeurbanne, France

2 Institute of Chemistry, São Paulo State University (UNESP), Araraquara, São Paulo, Brazil

3 Institute of Analytical Sciences, UMR 5280, Claude Bernard Lyon 1 University, University of Lyon, Villeurbanne, France

Silica (SiO<sub>2</sub>) nanoparticles have many valuable properties that make them a promising platform for nanomedicine development, becoming one of the most important materials in nanotechnology [18, 19]. They show an extensive surface area, biocompatibility, high chemical and colloidal stability, low-cost material, easy surface functionalization, optical transparency, and easy diffusion through the whole body. Moreover, size, shape, porosity and surface charge of silica nanoparticles are easily controlled. Further, silica coating on the surface of other nanoparticles is a common process of surface modification of nanoparticles [20–22].

Template deposition of silica into organic nanoparticles is a synthesis method used currently for controlling the porosity, size and shape of silica nanoparticles and hollow silica nanoparticles [23]. Also, it allows producing silica-organic hybrid nanoparticles (with a good control over the silica-organic material ratio) which have been received special attention due to their possible applications in the biomedical field [24–29]

On the other hand, bovine serum albumin (BSA) also represents a promising material when it comes to nanoparticle preparation for drug delivery. It is a natural protein that is readily available and relatively cheap to obtain. It is biocompatible, biodegradable, and does not produce undesired degradation products. The natural role of BSA is to work as transporter for various molecules in the blood. This function gives BSA the ability to bind to a wide range of molecules and therefore can serve as an excellent drug carrier. BSA-based nanoparticles were prepared, studied previously and proven to be a good carrier for a wide range of drugs and biomolecules [30, 31]. In addition, the lack of toxicity of BSA can also represent a great value to the obtained nanoparticles [32].

Several works can be found about nanomaterials production with BSA (or protein in general) and silica being the two main components [33, 34]. The presence of protein in the formulations can make silica particles less harmless and not taken up by macrophages [19]. In another study, it was suggested that BSA coating of silica nanoparticles may reduce their damage to biological cells and reduce their uptake by the immune system. BSA coated particles needed more time for membrane disruption than uncoated silica particles and therefore decrease the membrane damage by protein adsorption [35]. Furthermore, human serum albumin (HSA) coating of silica nanoparticles in a bilayer system consisting of HSA and poly(acrylic acid-*co*-itaconic acid) allowed a pH-responsive gemcitabine release and improved cytotoxicity in mouse fibroblast cells after 24 h of incubation [36]. Furthermore, it was reported the preparation silica nanoparticles in presence of BSA and polyethylenimine, in which BSA improved the size distribution of the obtained nanoparticles, however, the procedure did not involve the deposition of silica into BSA particles [37].

In this work, BSA-silica hybrid nanoparticles were synthesized through the deposition of silica into BSA nanoparticles. To our knowledge, no previous work was done on the matter since the formulation obtained was not a core-shell structure, instead, interpenetrated networks of the components. Moreover, the influence of TEOS and ammonia concentration on the particle properties were evaluated. This formulation can lead to a promising drug delivery system for in vivo administration.

## 2 Experimental

### 2.1 Materials and Reagents

Bovine serum albumin (BSA, 96%) was obtained from Sigma-Aldrich. Polyvinylpyrrolidone (PVP) and tetraethyl orthosilicate (TEOS) were purchased from Fluka. Glutaraldehyde (25%), ethanol (96%) and ammonia solutions (NH<sub>4</sub>OH, 25%) were purchased from VWR Prolabo and used as received.

### 2.2 BSA Nanoparticles (BSA-NP)

An aqueous BSA solution was prepared at a concentration of 20 mg/ml. BSA nanoparticles were obtained by adding ethanol to the BSA solution with a solvent/non-solvent ratio of 1/2 under magnetic stirring at room temperature. Upon ethanol addition, glutaraldehyde (8 wt% respect to BSA) was added as crosslinker and kept under magnetic stirring for 10 min. Ethanol was then removed by rotary evaporation (30°C, 100 rpm) and the BSA nanoparticles dispersed in water were recovered.

### 2.3 Preparation of BSA-Silica Hybrid Nanoparticles (BS)

A mass of 0.2 g of PVP was dissolved in 4 ml of BSA-NP aqueous suspension (2% w/v) and kept under magnetic agitation for 3 h. Then, ammonia (NH<sub>4</sub>OH) was added to the suspension. Afterwards, a solution of TEOS in ethanol (25% v/v) was added to the suspension and kept under magnetic agitation overnight. Hybrid nanoparticles were separated from the solution by centrifugation and redispersed in water by ultrasonication. This procedure was repeated five times for ensuring the removal of unreacted material. Different samples of BSA-silica hybrid nanoparticles were prepared by varying the quantity of ammonia and TEOS used in the preparation according to Table 1. The influence of ammonia and TEOS concentration on the physicochemical properties of the obtained nanoparticles were evaluated.

**Table 1** Quantities of ammonia and TEOS solutions used for preparing the samples

Sample	NH <sub>4</sub> OH (μL)	TEOS solution (25% v/v, μL)
BS1	280	160
BS2	280	320
BS3	280	480
BS4	160	480
BS5	400	480

## 2.4 Samples Characterization

FTIR analyses were performed by FTIR spectrophotometer Nicolet iS50 FTIR (Thermo Scientific) in the ATR mode. Nanoparticles suspension was dropped onto the ATR crystal and left to dry prior to analysis. The spectra were scanned over the range 4000–500 cm<sup>-1</sup>.

The surface charge of the nanoparticles was determined by measurements of zeta potential using Zetasizer Nano ZS equipment. Zeta potential was measured as a function of pH in the range 2.5–9.5 at room temperature. Nanoparticles were dispersed in 5 mmol l<sup>-1</sup> NaCl aqueous solution. Zeta potential was measured by taking an average of three measures.

Thermogravimetry Analysis (TGA) of dried samples was performed by TG 209 F1 ASC (Netzsch) equipment from 25 °C up to 1000 °C at a heating rate of 10 °C/min under a nitrogen flow rate of 20 ml/min.

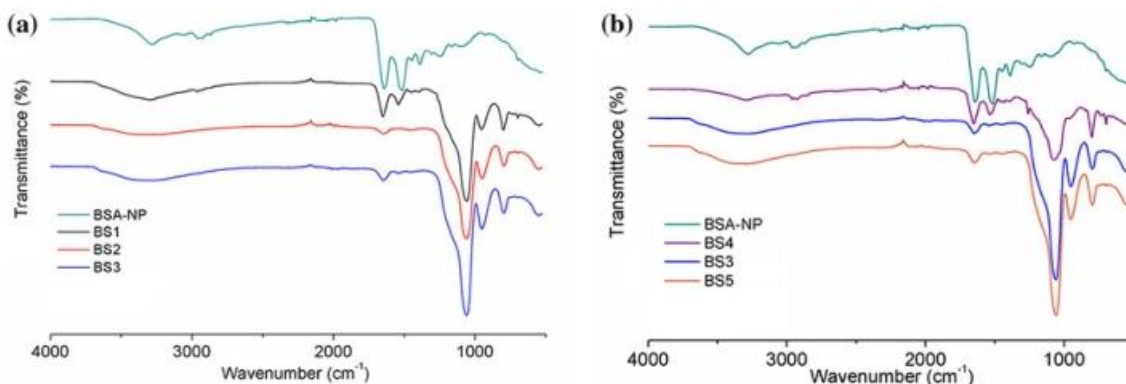
Transmission electron microscopy (TEM) images were obtained with a Phillips CM120 electron microscope (Claude Bernard University—Lyon1, CTμ, Lyon, France). One drop of highly diluted particles suspension was placed onto a copper grid (mesh 200 and covered with formvar-carbon) and dried at room temperature before TEM analysis. The analyses were performed with a field emission gun

operating at 100 kV. The average size and the standard deviation were calculated assuming a lognormal distribution of the particles size.

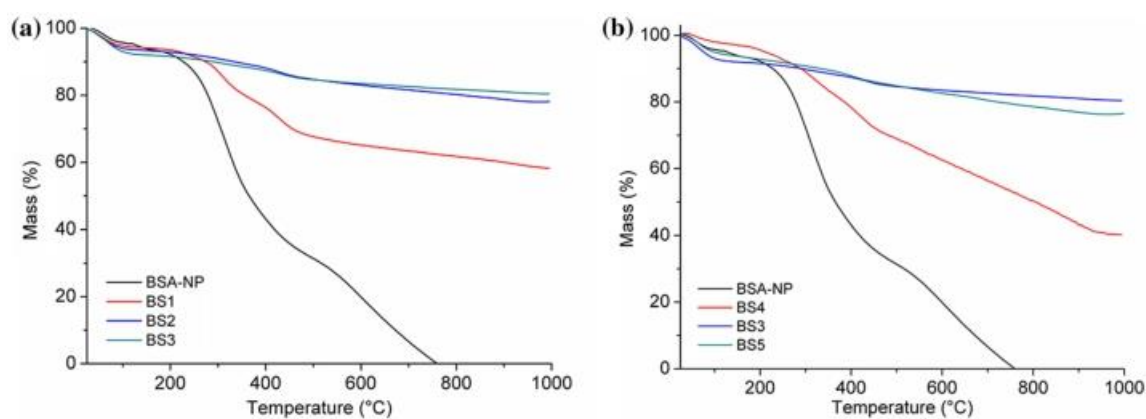
## 3 Results and Discussion

Figure 1 displays the FTIR spectra of the obtained samples. The BSA-NP spectrum exhibits bands at 1520 and 1645 cm<sup>-1</sup>, which are assigned to amide II and amide I vibration modes, respectively. These bands are produced by the presence of peptide bonds in the BSA protein. Bands at 3060 and 3280 cm<sup>-1</sup> are related to -NH and -OH stretching vibrations. Bands at 2960, 2930 and 2870 cm<sup>-1</sup> are associated to -CH stretching [38, 39]. These last bands confirm the organic nature of the examined material. All the BSA-silica hybrid nanoparticles (BS samples) present intense bands at 1060, 950 and 795 cm<sup>-1</sup> associated to the asymmetric stretching vibration of Si-O-Si, stretching vibration of Si-OH and symmetric stretching vibration of Si-O-Si, respectively, which confirms the presence of silica in these nanoparticles [40, 41]. BS1 and BS4 spectra present bands attributed to BSA and silica. However, BS2, BS3 and BS5 spectra do not exhibit bands related to BSA. Probably the concentration of BSA in BS2, BS3 and BS5 samples is so low that the bands related to BSA are not observable in the spectra.

TGA curves of BSA-NP, BS1, BS2, BS3, BS4 and BS5 nanoparticles are shown in Fig. 2. The weight losses in the range 25–200 °C are assigned to the loss of physically absorbed water. Above 200 °C, the weight losses are attributed to the decomposition of organic material, which is mainly albumin. The curve of the BSA-NP sample shows an abrupt mass drop near 300 °C and then a continuous decrease of mass to total calcination, which confirms that the BSA-NP sample is effectively formed by organic material. The BS nanoparticles decreased in mass with increasing



**Fig. 1** FTIR spectra: **a** samples prepared varying the TEOS concentration: BS1, BS2, BS3 and BSA-NP. **b** Samples prepared varying the ammonia concentration: BS4, BS3, BS5 and BSA-NP



**Fig. 2** TGA curves: **a** samples prepared by varying the TEOS concentration: BS1, BS2, BS3 and BSA-NP. **b** Samples prepared by varying the ammonia concentration: BS4, BS3, BS5 and BSA-NP

**Table 2** Characteristics of BSA nanoparticles (BSA-NP) and hybrid nanoparticles (BS): medium size, isoelectric point and silica content

Sample	Average size (nm)	Isoelectric point	Silica content (%)
BSA-NP	84 ± 10	5.0	0
BS1	134 ± 23	4.2	58.2
BS2	213 ± 15	4.0	78.0
BS3	219 ± 14	3.8	80.5
BS4	90 ± 13	4.7	40.0
BS5	251 ± 14	2.0	76.8

temperature due to the calcination of the organic material (BSA) inside. However, the final mass of the BS samples was nonzero, since these samples also contain silica, which does not decompose with increasing temperature. Consequently, the mass remaining after calcination corresponds to silica [38]. The silica content in BS nanoparticles is listed in Table 2. The high content of silica in BS2, BS3 and BS5 nanoparticles can also be interpreted as a low content of BSA, as it was suggested by the FTIR analysis. The TGA curves of samples BS1 and BS4 exhibited a slightly abrupt mass drop near 300 °C similar to the behaviour of the BSA-NP sample. However, the decrease of the mass above 200 °C in samples BS2, BS3 and BS5 was not abrupt otherwise continuous. These differences in the TGA curves of the BS samples were attributed to the silica content. The incorporation of inorganic material in an organic matrix usually promotes the thermal stability, that is, it delays the thermal decomposition process of the organic material which can be observed in the TGA curve as an increase of the decomposition temperature and as a less abrupt decrease of the mass [28, 42, 43]. This effect was observed in the TGA curves of the BS samples, where the samples with higher silica content showed a slow and continuous decrease of the mass.

Because TEOS is the source of silica and the presence of ammonia increases the rate of hydrolysis and condensation reactions, increasing the concentration of ammonia or TEOS should increase the amount of generated silica. Thus, more silica would be available to be incorporated into the albumin nanoparticles resulting in hybrid nanoparticles BS with higher content of silica. The TGA results reveal the increase in silica content when TEOS concentration is increased in the synthesis of BSA-silica hybrid nanoparticles, which was expected as discussed above. A similar tendency was expected for the influence of ammonia concentration in the silica content. BS3 has larger silica content than BS4, which agrees with the previous assumption that suggests an increase in the silica content when the ammonia concentration increases. Although the concentration of ammonia was greater in BS5 than in BS3 (Table 1), the silica content in BS5 was lower than in BS3 (Table 2). Despite silica is a chemically stable material in solutions with low pH and in neutral solutions, its solubility in alkaline solutions increases with increasing pH [44, 45].

The BS3 and BS5 nanoparticles were prepared with the same amount of TEOS, that is, the amount of silica generated to be incorporated into the nanoparticles would be equal if the synthetic conditions were similar. However, the amount of ammonia used in the synthesis of BS5 was higher than in BS3 (Table 1), so the final pH of the solution was higher in BS5. Probably, the higher pH in the BS5 suspension compared to that of BS3 suspension promoted the dissolution of a part of the silica generated, decreasing the amount of silica that was incorporated into the BSA-NP.

Zeta potential curves of BSA-NP, BS1, BS2, BS3, BS4 and BS5 nanoparticles as a function of pH are displayed in Fig. 3. The zeta potential curve depends on the physico-chemical features of the nanoparticles surface; thus, it supplies information about the chemical species on the nanoparticles surface. All samples exhibit the typical profile of

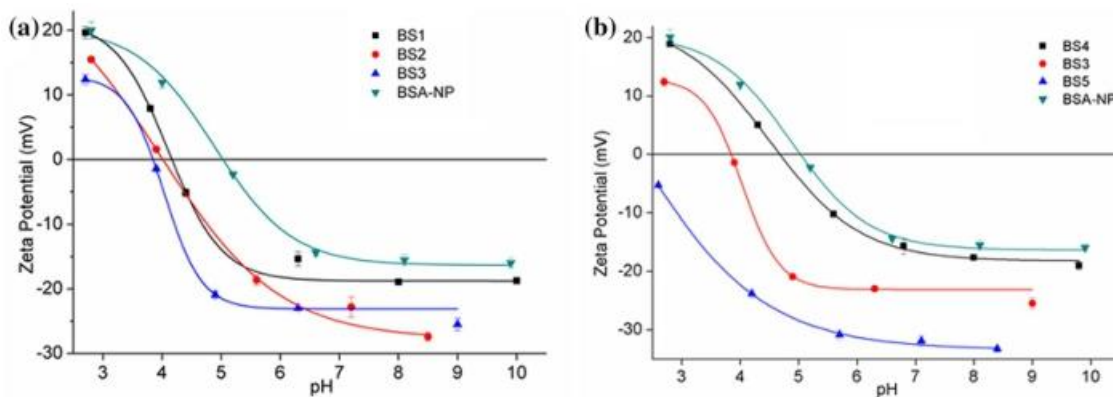


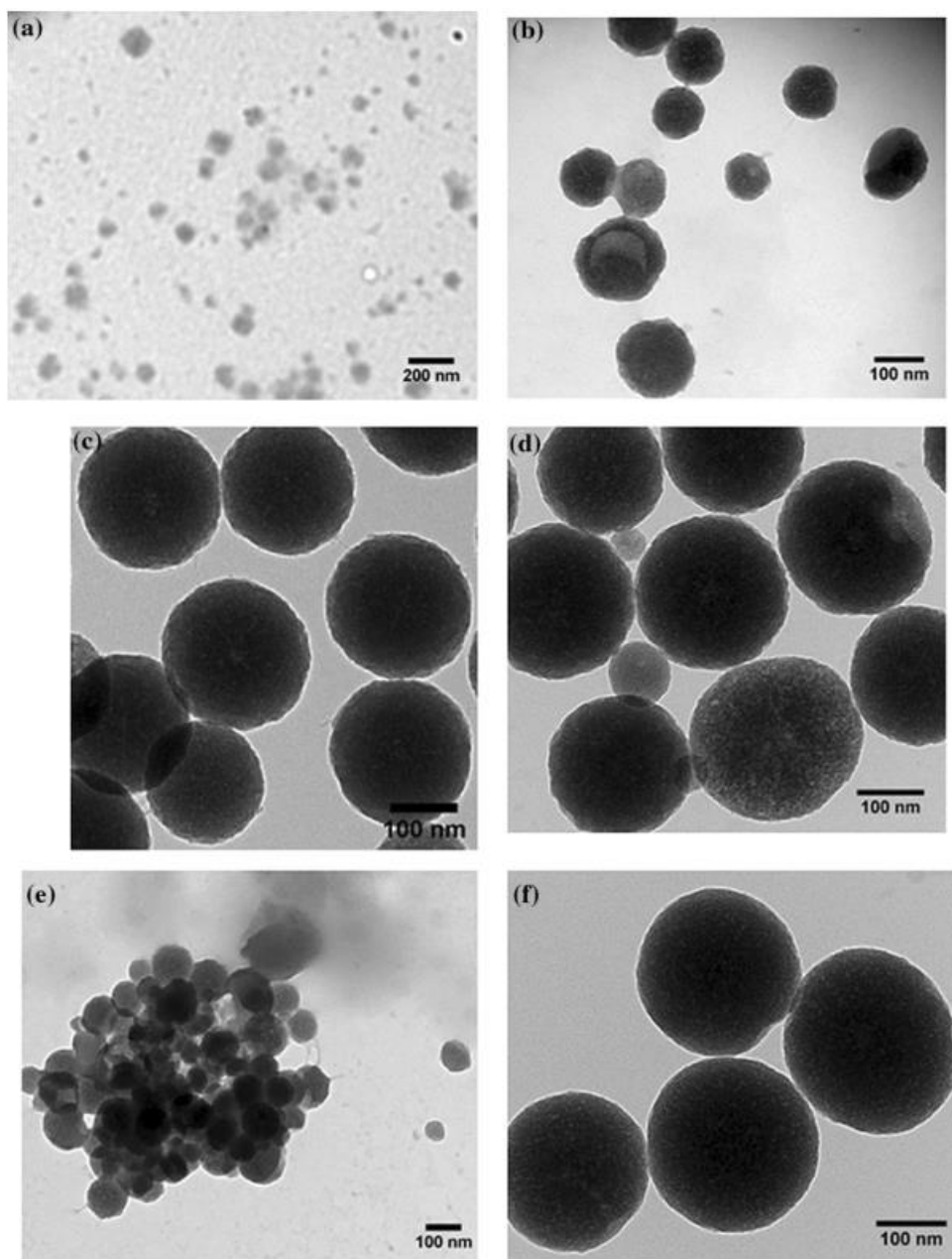
**Fig. 3** Zeta potential as a function of pH: **a** samples prepared by varying the TEOS concentration: BS1, BS2, BS3 and BSA-NP. **b** Samples prepared by varying the ammonia concentration: BS4, BS3, BS5 and BSA-NP

zeta potential curve; however, the isoelectric point (IEP, i.e. pH at which zeta potential is zero) is different for each sample. The values of IEP are listed in Table 2. The IEP of BSA-NP is 5.0, which agrees with the reported value in previous works [39, 46]. Nanoparticles with core-shell structure in which the shell is formed exclusively by silica have a zeta potential curve similar to the curve of silica nanoparticles and an IEP around 2.0 [47, 48]. The IEP of BS1, BS2, BS3 and BS4 nanoparticles is lower than the IEP of BSA-NP and higher than that of silica, so it seems reasonable to assume that silica and BSA are present on the surface of these nanoparticles and the proportion of these materials determines the IEP of each sample [25, 49]. The zeta potential curve of BS4 nanoparticles is similar to that of BSA-NP nanoparticles, also their IEP are slightly similar. These results suggest that the surface of BS4 nanoparticles is composed mainly of BSA. Although the silica content on the surface of the BS4 nanoparticles is low, the results of the thermogravimetric analysis (Table 2) suggest that BS4 nanoparticles are formed by 40% of silica, so the silica is also distributed inside the nanoparticle. The zeta potential curve of the sample BS5 is similar to that of silica nanoparticles. Although the measured zeta potential values of the BS5 sample were below 0 mV, the IEP of the nanoparticles was estimated at about 2.0, which is similar to the IEP of silica. The IEP of BS5 suggests a high concentration of silica on the surface of the nanoparticles, therefore it is possible that BS5 nanoparticles present a layer composed almost exclusively of silica on the surface of the nanoparticles. An increase in TEOS or ammonia concentration produces a reduction in the IEP of BS nanoparticles because it raises the silica content on the surface of BS nanoparticles. These results indicate that the IEP of BSA-silica hybrid nanoparticles could be adjusted between 5 and 2 by tuning the concentration of the reagents adequately.

It is important to mention that the choice of ammonia volumes for this experiment was based on the results of a previous study of ours in which it was found that crosslinked BSA nanoparticles are resistant to pH increase until pH 11 [30]. The amount of ammonia used here did not exceed the amount of ammonia used in the cited study, and therefore, the integrity of BSA nanoparticles during preparation is guaranteed.

TEM images of BSA-NP, BS1, BS2, BS3, BS4 and BS5 nanoparticles are shown in Fig. 4. TEM images verify the presence of homogeneous nanoparticles with a porous surface. Since no core-shell structure was observed in BS nanoparticles, apparently, silica was deposited into the albumin nanoparticles. Moreover, there was no evidence of nontemplated silica nanoparticles. The average size and the standard deviation of the nanoparticles are presented in Table 2. These results show that the nanoparticles have monodisperse size distributions. BSA nanoparticles (BSA-NP) were prepared by the nanoprecipitation method. When ethanol was added to the aqueous solution of BSA, the solubility of BSA in water decreased and the molecules precipitated forming agglomerates of BSA, which were cross-linked with glutaraldehyde to forming BSA-NP. The BSA-silica hybrid nanoparticles (BS) were obtained via the template deposition of silica into preformed BSA-NP. Silica was produced from TEOS by the sol-gel process. Hydrolysis of TEOS in water produced silanols, afterwards, condensation of silanols produced first oligomers and then silica primary nuclei. Since BSA nanoparticles present a porous structure, silica precursors penetrate easily into the nanoparticles, then, nucleation and assembly of silica take place inside the nanoparticles [27]. It seems that BSA provides an environment that facilitates silica nucleation and growth of the particles, probably due to the functional groups of BSA that could associate with silica through hydrogen bonding and electrostatic interactions [50]. During the growth of silica, BSA protein

**Fig. 4** TEM images: **a** BSA-NP. BSA-silica hybrid nanoparticles: **b** BS1, **c** BS2, **d** BS3, **e** BS4 and **f** BS5



is entrapped into the silica framework. BSA-NP morphology is slightly irregular (Fig. 4a). A similar morphology but closer to a sphere is observed in samples BS1 (Fig. 4b) and BS4 (Fig. 4e), while the nanoparticles BS2 (Fig. 4c), BS3 (Fig. 4d) and BS5 (Fig. 4f) are approximately spherical. These differences are probably due to the amount of silica in the BS nanoparticles. BSA-NP nanoparticles store water in their structure when they are in aqueous suspension. The volume and shape depend on the amount of water stored. During the drying process, the BSA-NP nanoparticles loss water, decreasing in volume and producing dry nanoparticles with slightly different shapes. Silica in the BS nanoparticles results in an inorganic matrix that confers stiffness to the

nanoparticles. The loss of water during drying does not alter the shape of the inorganic matrix and maintains almost the same shape when they are suspended or dried. Therefore, the BS nanoparticles are less altered by shrinkage during the drying process than the BSA-NP [25]. This effect depends on the amount of silica in the nanoparticles. Nanoparticles with less silica, such as BS1 and BS4 (Table 2) are slightly modified by the drying process. Such nanoparticles appear in TEM images as slightly irregular spheres. Whereas, BS2, BS3 and BS5 nanoparticles, composed of more than 75% silica, are not affected by the drying process and maintain a spherical shape even after drying. The concentration of TEOS and ammonia in the synthesis of BSA-silica hybrid

nanoparticles influences significantly the average size of the nanoparticles. An increase in the TEOS or ammonia concentration (in the working range) produced bigger nanoparticles. This tendency was also observed in previous articles related to the synthesis of silica nanoparticles [26, 51, 52]. As discussed previously, an increase in TEOS or ammonia concentration raises the formation of silica, thus more silica is available for being incorporated into the albumin nanoparticles producing bigger BS nanoparticles. This relationship was confirmed by the TGA results in samples BS1, BS2, BS3 and BS4. That is, the size of the nanoparticles depends on the amount of silica available to be incorporated into the BSA-NP nanoparticles. Although the average size of BS5 nanoparticles is larger than that of other BS nanoparticles, BS5 nanoparticles do not have the highest silica content among BS nanoparticles (Table 2). Probably, on the BS5 nanoparticles, the silica network did not penetrate as deeply into the BSA-NP nanoparticles as other BS nanoparticles, thus having more silica to be incorporated into the surface and allowing the growth of a silica shell as indicated by the results of zeta potential. However, it is unclear the reason for the different silica distribution in BS5, a more extensive study is necessary to elucidate the phenomenon.

Hybrid nanoparticles possess the trait of being multifunctional according to their main compositions. Therefore, it is important to understand and control the distribution and amount of their components within the system. This can highlight one function on top of the other and lead to more sophisticated profile of applications [10]. In addition, controlling the physico-chemical properties of the particles such as size, charge, and morphology, is known to be crucial for any biomedical and biotechnological applications, therein lies the importance of this work. Indeed, other relevant synthesis parameters to produce BSA-silica hybrid nanoparticles as the degree of cross-linking of BSA nanoparticles [53], size of BSA-based nanoparticles [30], reaction temperature [54], and degradation behaviour [55] would be considered in a future work.

## 4 Conclusion

In this work, BSA-silica hybrid nanoparticles were synthesized via the template deposition of silica into BSA nanoparticles. The silica was produced through the sol-gel process and embedded in the BSA nanoparticles. It was found that the method is able to produce monodisperse hybrid nanoparticles. The effect of TEOS and ammonia concentration on the properties of nanoparticles was investigated. The results suggest that the particles size, isoelectric point and silica content of the hybrid nanoparticles can be easily tuned by controlling adequately the concentration of TEOS and ammonia. In general, an increase in TEOS or

ammonia concentration increases the size and silica content and decreases the isoelectric point. To our knowledge, this is the first work that reports the synthesis of BSA-silica hybrid nanoparticles in a non-core-shell structure.

**Acknowledgements** Jaime Vega-Chacón would like to thank Coordenação de aperfeiçoamento de Pessoal de Nivel Superior (CAPES) for the grant funded Bolsista capes/Programa Doutorado Sanduiche no Exterior/Processo no. (88881.132878/2016-01). The authors would like to thank Campus France for supporting this project with the grant PHC PROCOPE Project ID: 57129895. We also thank the European Research Council for their funding under the European Union's Horizon 2020 research and innovation programme under Grant Agreement No. 643694.

## References

1. Panda MK, Panda SK, Singh YD, Jit BP, Behara RK, Dhal NK (2020) Role of nanoparticles and nanomaterials in drug delivery: an overview. *Advance pharmacy biotechnology*. Springer, Singapore, pp 247–265
2. Jeevanandam J, Pal K, Danquah MK (2019) Virus-like nanoparticles as a novel delivery tool in gene therapy. *Biochimie* 157:38–47
3. Luangtana-anan M, Nunthanid J, Limmatvapirat S (2019) Potential of different salt forming agents on the formation of chitosan nanoparticles as carriers for protein drug delivery systems. *J Pharm Investig* 49:37–44
4. Mie M, Matsumoto R, Mashimo Y, Cass AEG, Kobatake E (2019) Development of drug-loaded protein nanoparticles displaying enzymatically-conjugated DNA aptamers for cancer cell targeting. *Mol Biol Rep* 46:261–269
5. Chen T, Cen D, Ren Z, Wang Y, Cai X, Huang J, Di Silvio L, Li X, Han G (2019) Bismuth embedded silica nanoparticles loaded with autophagy suppressant to promote photothermal therapy. *Biomaterials* 221:119419
6. Soleymani M, Velashjerdi M, Shaterabadi Z, Barati A (2020) One-pot preparation of hyaluronic acid-coated iron oxide nanoparticles for magnetic hyperthermia therapy and targeting CD44-overexpressing cancer cells. *Carbohydr Polym* 237:116130
7. Duse L, Agel MR, Pinnapireddy SR, Schäfer J, Selo MA, Ehrhardt C, Bakowsky U (2019) Photodynamic therapy of ovarian carcinoma cells with curcumin-loaded biodegradable polymeric nanoparticles. *Pharmaceutics* 11:282
8. Paysen H, Loewa N, Weber K, Kosch O, Wells J, Schaeffter T, Wiekhorst F (2019) Imaging and quantification of magnetic nanoparticles: Comparison of magnetic resonance imaging and magnetic particle imaging. *J Magn Magn Mater* 475:382–388
9. Xu X, Li H, Li K, Zeng Q, Liu Y, Zeng Y, Chen D, Liang J, Chen X, Zhan Y (2019) A photo-triggered conjugation approach for attaching RGD ligands to biodegradable mesoporous silica nanoparticles for the tumor fluorescent imaging. *Nanomed Biol Med* 19:136–144
10. Marcelo GA, Lodeiro C, Capelo JL, Lorenzo J, Oliveira E (2020) Magnetic, fluorescent and hybrid nanoparticles: from synthesis to application in biosystems. *Mater Sci Eng C*. <https://doi.org/10.1016/j.msec.2019.110104>
11. Parveen S, Misra R, Sahoo SK (2012) Nanoparticles: a boon to drug delivery, therapeutics, diagnostics and imaging. *Nanomedicine* 8:147–166
12. Biju V (2014) Chemical modifications and bioconjugate reactions of nanomaterials for sensing, imaging, drug delivery and therapy. *Chem Soc Rev* 43:744–764

13. Wang R, Billone PS, Mullett WM (2013) Nanomedicine in action: an overview of cancer nanomedicine on the market and in clinical trials. *J Nanomater* 2013:1–12
14. Hood M, Mari M, Muñoz-Espí R (2014) Synthetic strategies in the preparation of polymer/inorganic hybrid nanoparticles. *Materials (Basel)* 7:4057–4087
15. Sailor MJ, Park J-H (2012) Hybrid nanoparticles for detection and treatment of cancer. *Adv Mater* 24:3779–3802
16. Elzoghby AO, Hemasa AL, Freag MS (2016) Hybrid protein-inorganic nanoparticles: from tumor-targeted drug delivery to cancer imaging. *J Control Release* 243:303–322
17. Liu J, Detrembleur C, Mornet S, Jérôme C, Duguet E (2015) Design of hybrid nanovehicles for remotely triggered drug release: an overview. *J Mater Chem B* 3:6117–6147
18. Saroj S, Rajput SJ (2018) Composite smart mesoporous silica nanoparticles as promising therapeutic and diagnostic candidates: recent trends and applications. *J Drug Deliv Sci Technol* 44:349–365
19. Bagheri E, Ansari L, Abnous K, Taghdisi SM, Charbgo F, Ramezani M, Alibolandi M (2018) Silica based hybrid materials for drug delivery and bioimaging. *J Control Release* 277:57–76
20. Liberman A, Mendez N, Trogler WC, Kummel AC (2014) Synthesis and surface functionalization of silica nanoparticles for nanomedicine. *Surf Sci Rep* 69:132–158
21. Guerrero-Martínez A, Pérez-Juste J, Liz-Marzán LM (2010) Recent progress on silica coating of nanoparticles and related nanomaterials. *Adv Mater* 22:1182–1195
22. Vivero-Escoto JL, Slowing IL, Trewyn BG, Lin VS-Y (2010) Mesoporous silica nanoparticles for intracellular controlled drug delivery. *Small* 6:1952–1967
23. Petry R, Saboia VM, Franqui LS, de Holanda C, Garcia de TRR, Farias MA, de Souza Filho AG, Ferreira OP, Martinez DST, Paula AJ (2019) On the formation of protein corona on colloidal nanoparticles stabilized by depletant polymers. *Mater Sci Eng C* 105:110080
24. McInnes SJP, Voelcker NH (2009) Silicon-polymer hybrid materials for drug delivery. *Future Med Chem* 1:1051–1074
25. Zhou F, Li S, Vo CD, Yuan JJ, Chai S, Gao Q, Armes SP, Lu C, Cheng S (2007) Biomimetic deposition of silica templated by a cationic polyamine-containing microgel. *Langmuir* 23:9737–9744
26. Pi M, Yang T, Yuan J, Fujii S, Kakigi Y, Nakamura Y, Cheng S (2010) Biomimetic synthesis of raspberry-like hybrid polymer-silica core-shell nanoparticles by templating colloidal particles with hairy polyamine shell. *Colloids Surf B Biointerfaces* 78:193–199
27. Zhang J, Jia J, Kim JP, Yang F, Wang X, Shen H, Xu S, Yang J, Wu D (2018) Construction of versatile multilayered composite nanoparticles from a customized nanogel template. *Bioact Mater* 3:87–96
28. Wang J, Yang S, Li C, Miao Y, Zhu L, Mao C, Yang M (2017) Nucleation and assembly of silica into protein-based nanocomposites as effective anticancer drug carriers using self-assembled silk protein nanostructures as biotemplates. *ACS Appl Mater Interfaces* 9:22259–22267
29. Li Z, Chen T, Nie J, Xu J, Fan Z, Du B (2013) P(NIPAm-co-TMSPMA)/silica hybrid microgels: structures, swelling properties and applications in fabricating macroporous silica. *Mater Chem Phys* 138:650–657
30. Tarhini M, Benlyamani I, Hamdani S, Agusti G, Fessi H, Greige-Gerges H, Bentaher A, Elaissari A (2018) Protein-based nanoparticle preparation via nanoprecipitation method. *Materials (Basel)* 11:394–412
31. Martínez Rivas CJ, Tarhini M, Badri W, Miladi K, Greige-Gerges H, Nazari QA, Galindo Rodríguez SA, Román RÁ, Fessi H, Elaissari A (2017) Nanoprecipitation process: from encapsulation to drug delivery. *Int J Pharm* 532:66–81
32. Tarhini M, Greige-Gerges H, Elaissari A (2017) Protein-based nanoparticles: from preparation to encapsulation of active molecules. *Int J Pharm* 522:172–197
33. Chrzanowska A, Derylo-Marczewska A (2019) Mesoporous silica/protein biocomposites: Surface, topography, thermal properties. *Int J Biol Macromol* 139:531–542
34. Zampini G, Matino D, Quaglia G, Tarpani L, Gargaro M, Cecchetti F, Iorio A, Fallarino F, Latterini L (2019) Experimental evidences on the role of silica nanoparticles surface morphology on the loading, release and activity of three proteins. *Microporous Mesoporous Mater* 287:220–227
35. Wei X, Qu X, Ding L, Hu J, Jiang W (2016) Role of bovine serum albumin and humic acid in the interaction between SiO<sub>2</sub> nanoparticles and model cell membranes. *Environ Pollut* 219:1–8
36. Pourjavadi A, Tehrani ZM (2016) Mesoporous silica nanoparticles with bilayer coating of poly(acrylic acid-co-itaconic acid) and human serum albumin (HSA): a pH-sensitive carrier for gemcitabine delivery. *Mater Sci Eng C* 61:782–790
37. Jackson E, Ferrari M, Cuestas-Ayllon C, Fernández-Pacheco R, Perez-Carvajal J, de la Fuente JM, Grazú V, Betancor L (2015) Protein-templated biomimetic silica nanoparticles. *Langmuir* 31:3687–3695
38. Li Z, Qiang L, Zhong S, Wang H, Cui X (2013) Synthesis and characterization of monodisperse magnetic Fe<sub>3</sub>O<sub>4</sub>@BSA core-shell nanoparticles. *Colloids Surf A Physicochem Eng Asp* 436:1145–1151
39. Qasim M, Asghar K, Dharmapuri G, Das D (2017) Investigation of novel superparamagnetic Ni<sub>0.5</sub>Zn<sub>0.5</sub>Fe<sub>2</sub>O<sub>4</sub>@albumen nanoparticles for controlled delivery of anti-cancer drug. *Nanotechnology* 28:365101
40. Katumba G, Mwakikunga BW, Mothibinyane TR (2008) FTIR and Raman spectroscopy of carbon nanoparticles in SiO<sub>2</sub>, ZnO and NiO matrices. *Nanoscale Res Lett* 3:421–426
41. Panwar K, Jassal M, Agrawal AK (2015) In situ synthesis of Ag-SiO<sub>2</sub> Janus particles with epoxy functionality for textile applications. *Particuology* 19:107–112
42. Geng H, Peng R, Han S, Gu X, Wang M (2010) Surface-modified titania nanoparticles with conjugated polymer for hybrid photo-voltaic devices. *J Electron Mater* 39:2346–2351
43. He Y (2004) Preparation of polyaniline/nano-ZnO composites via a novel Pickering emulsion route. *Powder Technol* 147:59–63
44. Maraghechi H, Rajabipour F, Pantano CG, Burgos WD (2016) Effect of calcium on dissolution and precipitation reactions of amorphous silica at high alkalinity. *Cem Concr Res* 87:1–13
45. Alexander GB, Heston WM, Iler RK (1954) The solubility of amorphous silica in water. *J Phys Chem* 58:453–455
46. Lu X, Wu J, Huo G, Sun Q, Huang Y, Han Z, Liang G (2012) Protein-passivated FeNi<sub>3</sub> particles with low toxicity and high inductive heating efficiency for thermal therapy. *Colloids Surf A Physicochem Eng Asp* 414:168–173
47. Wilhelm P, Stephan D (2006) On-line tracking of the coating of nanoscaled silica with titania nanoparticles via zeta-potential measurements. *J Colloid Interface Sci* 293:88–92
48. Souza DM, Andrade AL, Fabris JD, Valério P, Góes AM, Leite MF, Domingues RZ (2008) Synthesis and in vitro evaluation of toxicity of silica-coated magnetite nanoparticles. *J Non Cryst Solids* 354:4894–4897
49. Li X, Yuan J, Liu H, Jiang L, Sun S, Cheng S (2010) Microgel-silica hybrid particles: strategies for tunable nanostructure, composition, surface property and porphyrin functionalization. *J Colloid Interface Sci* 348:408–415
50. Fournier AC, McGrath KM (2011) Porous protein-silica composite formation: Manipulation of silicate porosity and protein conformation. *Soft Matter* 7:4918–4927
51. Rahman IA, Vejayakumaran P, Sipaut CS, Ismail J, Bakar MA, Adnan R, Chee CK (2007) An optimized sol-gel synthesis of

- 
- stable primary equivalent silica particles. *Colloids Surf A Physicochem Eng Asp* 294:102–110
52. Rao KS, El-Hami K, Kodaki T, Matsushige K, Makino K (2005) A novel method for synthesis of silica nanoparticles. *J Colloid Interface Sci* 289:125–131
53. Gupta MN, Perwez M, Sardar M (2020) Protein crosslinking: Uses in chemistry, biology and biotechnology. *Biocatal Biotransformation* 38:178–201
54. Yu E, Lo A, Jiang L, Petkus B, Ileri Ercan N, Stroeve P (2017) Improved controlled release of protein from expanded-pore mesoporous silica nanoparticles modified with co-functionalized poly(*n*-isopropylacrylamide) and poly(ethylene glycol) (PNIPAM-PEG). *Colloids Surf B Biointerfaces* 149:297–300
55. Vlasenkova MI, Dolinina ES, Parfenyuk EV (2019) Preparation of mesoporous silica microparticles by sol–gel/emulsion route for protein release. *Pharm Dev Technol* 24:243–252